Solid State Electrochemical Study of Phase Equilibria and Thermodynamics of the Ternary System Y-Fe-O at Elevated Temperatures

W. Piekarczyk *, W. Weppner, and A. Rabenau

Max-Planck-Institut für Festkörperforschung, Heisenbergstr. 1, D-7000 Stuttgart 80, FRG

Z. Naturforsch. **34a**, 430–436 (1979); received January 24, 1979

A solid state galvanic cell technique has been employed to determine the phase diagram of the ternary system Y–Fe–O in the temperature range from 900 to 1250 °C. Only electrical quantities need to be measured and the samples do not have to be quenched. $YFeO_3$ and $Y_3Fe_5O_{12}$ exist over the entire temperature range, whereas the third ternary compound YFe_2O_{4-x} is only thermodynamically stable above 1010 ± 9 °C. Above 1078 ± 15 °C YFe_2O_{4-x} comes into equilibrium with Y_2O_3.

With the same experimental arrangement the standard Gibbs free energies of formation ΔG_f^0 of the ternary compounds $YFeO_3$, $Y_3Fe_5O_{12}$ and YFe_2O_4 have been determined to be $-1366.0 + 0.2525 \times T$ kJ/mol $(1173 \leqq T\,[K] \leqq 1523)$, $-4912.2 + 0.9990 \times T$ kJ/mol $(1173 \leqq T[K] \leqq 1523)$ and $-1615.9 + 0.3068 \times T$ kJ/mol $(1283 \leqq T[K] \leqq 1523)$ as functions of the temperature, respectively.

I. Introduction

Several ternary compounds of the system Y-Fe-O have interesting magnetic properties and are therefore of great technological importance for applications such as microwave devices and in magnetic bubble and magneto-optic elements. In spite of this fact, fundamental properties concerning phase equilibria and thermodynamic data are unsufficiently known. This information is essential, however, to properly control the conditions for the growth of single crystals and the formation of the compounds during sintering.

Previously, phase studies have been performed by annealing samples of various Fe:Y-ratios in air [1–3], in pure oxygen [4–5] and in one case in pure CO_2 [4]. Van Hook [2, 4] has in addition measured the weight losses of the samples in order to determine their oxygen contents. Recently, Kimizuka and Katsura [6] have studied the phase equilibria with the help of thermogravimetric measurements under defined oxygen partial pressures at a fixed temperature of 1200 °C. On the basis of these measurements one part of the phase diagram bounded by the triangle Y_2O_3-Fe_2O_3-Fe has been constructed. Tretyakov et al. [7] have measured the oxygen equilibrium pressure over Y_2O_3-$YFeO_3$-Fe mixtures in the temperature range from 900 to 1100 °C.

In a preceding paper [8] we have investigated the dissociation pressures of $Y_3Fe_5O_{12}$ and $YFeO_3$ in the temperature range from 900 to 1250 °C by EMF measurements using a solid state galvanic cell technique. On the basis of these measurements, the standard Gibbs (free) energies, enthalpies, and entropies of formation of $Y_3Fe_5O_{12}$ and $YFeO_3$ from metallic iron, yttria (Y_2O_3) and oxygen were calculated.

A recently developed generally applicable electrochemical technique [9–11] allows the determination of the complete phase diagrams of ternary systems and thermodynamic data related to the formation of all existing compounds in an experimentally very tractable and precise manner. Only measurements of electrical quantities are involved and it is also possible to study materials which cannot be quenched. This method has been employed to study the phase equilibria in the ternary system Y-Fe-O in the temperature range from 900 to 1250 °C.

2. Experimental and General Considerations

The solid state galvanic cell employed in this study is shown schematically in Figure 1. Stabilized zirconia is used as a solid electrolyte for oxygen ions for determining the oxygen activity of the sample and also for varying its oxygen content by precisely known amounts upon passing a current through the cell. Porous Pt/air or in some cases a two-phase mixture of $Fe + Fe_{1-y}O$ were used as oxygen sources or sinks with well defined oxygen reference activities.

* On leave from the Institute of Physics, Polish Academy of Sciences, Warsaw, Poland.

Reprint requests to Dr. W. Weppner. Please order a reprint rather than making your own copy.

0340-4811 / 79 / 0400-0430 $ 01.00/0

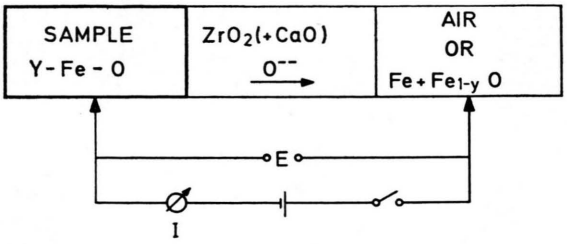

Fig. 1. Schematic representation of the galvanic cell used in this investigation and the electrical circuit.

Samples of various Y:Fe ratios were prepared in a similar manner to the procedure described previously [8]. Mixtures of Y_2O_3 — 99.99% (Alfa Products, Ventron) and Fe_2O_3 — Specpure (Johnson, Matthey & Co.) were used.

Depending on the direction of the current we have been able to oxidize or to reduce the sample. The compositions covered by the electrochemical variation of the oxygen content are located along the lines connecting the pure oxygen corner and the oxygen-free composition on the Y-Fe side of the Gibbs triangle of Y-Fe-O [11]. The steady state equilibrium cell voltage E is recorded as a function of the oxygen content. It is related to the oxygen activity a_0 or the oxygen equilibrium pressure p_{O_2} of the sample by Nernst's equation

$$E = \frac{RT}{2F} \ln \frac{a_0(\text{ref. electrode})}{a_0(\text{sample})} = \frac{RT}{4F} \ln \frac{p_{O_2}(\text{ref. electrode})}{p_{O_2}(\text{sample})}, \quad (1)$$

where R, T, and F are the universal gas constant (8.31441 J/mol · K), the absolute temperature and Faraday's constant (96484.56 C/mol), respectively.

According to Gibbs' phase rule, the cell voltage is independent of the oxygen content in the presence of three co-existing solid phases and may be expressed by their standard Gibbs energies of formation ΔG_f^0 (per mole)

$$E = \frac{1}{2F\,d} \sum_{i=1}^{3} (-1)^i\, d_{i3}\, \Delta G_f^0(Y_{\alpha_i}Fe_{\beta_i}O_{\gamma_i}) \quad (2)$$

where d is the determinant formed by the stoichiometric numbers of the three compounds,

$$d = \begin{vmatrix} \alpha_1 & \beta_1 & \gamma_1 \\ \alpha_2 & \beta_2 & \gamma_2 \\ \alpha_3 & \beta_3 & \gamma_3 \end{vmatrix}. \quad (3)$$

d_{i3} is the minor of d, which is formed by eliminating the third row (i.e., the stoichiometric numbers of the conducting oxygen species) and the i-th line of the determinant d.

Using Eq. (2), the Gibbs energies and related thermodynamic properties of all compounds existing in the system may be evaluated.

A voltage change with oxygen concentration has to be observed in 2- and 1-phase regions which separate 3-phase regions from each other (gaseous phases are disregarded in these considerations). The voltage (with reference to a pure oxygen electrode) has to decrease with increasing oxygen content of the sample and the plot of the cell voltage against the oxygen content has a step-like shape. The phase diagram may be identified in this way [11].

For studying variations of the phase diagram with temperature it is usually sufficient to determine the equilibrium cell voltages of the 3-phase regions as functions of the temperature. A change in the phase diagram would produce a break in the linear voltage versus temperature plot.

It is essential that all oxygen added to or taken from the sample is quantitatively determined by the charge flux in the external circuit. The transport of uncharged oxygen through the gas phase or the solid electrolyte (i.e., if electrons or holes are simultaneously moving with the oxygen ions) has to be negligibly small. For this purpose, tubes made from the electrolyte material with separated inside and outside electrode compartments were used. The parts covered with porous platinum served as electrolytes. In order to reduce oxygen permeation, a double walled tube arrangement was chosen which is shown in Figure 2. The voltage across the inner tube was always kept at zero during the equilibration of the sample with the help of a potentiostat (Lead 3 is connected to the reference, 4 and 5 to the working and 6 to the counter electrode output). Any deviation of the oxygen partial pressure in the space between the tubes from the equilibrium partial pressure of the sample is then eliminated by a current flow through the outer tube. This removes any driving force for the permeation of oxygen. For the change of the oxygen content of the sample, oxygen has to pass through both tubes and across the gaseous gap between.

Alternatively and in order to test the new measurement technique we have also performed some measurements with the help of an arrangement which is shown in Figure 3. Using this arrangement we have measured the oxygen equilibrium pressures

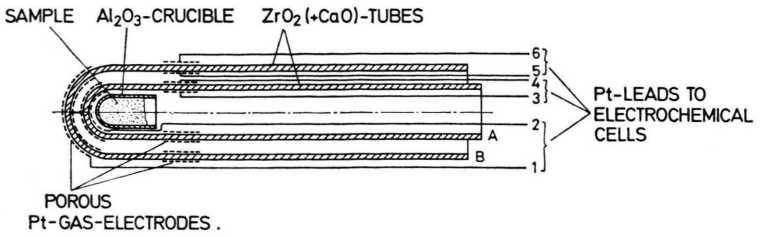

Fig. 2. The experimental galvanic cell with a double tube solid electrolyte and an air reference electrode which also acts as an oxygen sink or source.

of those 3-phase regions which have oxygen activities close to $Fe + Fe_{1-y}O$ mixtures. The space in-between the ZrO_2 (+ CaO) tubes was filled with Fe and $Fe_{1-y}O$ in this case. Due to the small gradient of the oxygen activity across the inner tube, the oxygen permeation was decreased to a very small level.

3. Results

3.1. Phase Diagram

In Fig. 4, the logarithm of the oxygen partial pressure as calculated using Eq. (1) from the observed voltages for the various 3-phase regions is plotted against the reciprocal of the absolute temperature. The data have been treated by the least squares (linear regression) method. For comparison the results obtained by Kimizuka and Katsura [6] and Tretyakov et al. [7] are also included.

The straight lines shown in Fig. 4 belong to the 3-phase regions as listed in Table 1. The values x', x'', x''', y', y'', and y''' represent specific deviations from the ideal stoichiometry of the compounds YFe_2O_{4-x} and $Fe_{1-y}O$.

The corresponding experimentally observed composition independent oxygen equilibrium pressures of these 3-phase regions may be expressed by Eqs. (4)—(10) which are included in Table 1.

Table 1. Compilation of the investigated 3-phase regions of the ternary system Y-Fe-O and their equilibrium oxygen partial pressures.

3-phase region of the ternary system Y-Fe-O	Logarithm of the oxygen equilibrium partial pressure, $\log p_{O_2}$ [Pa]	
A $Fe–Y_2O_3–YFeO_3$	$-\frac{29345}{T} + 13.00 \pm 0.04$	(4)
B $Fe–Y_2O_3–YFe_2O_{4-x'}$	$-\frac{28685}{T} + 12.53 \pm 0.04$	(5)
C $Fe–Fe_{1-y'}O–YFeO_3$	$-\frac{27855}{T} + 12.03 \pm 0.04$	(6)
D $Fe–Fe_{1-y'}O–YFe_2O_{4-x''}$		
E Y_2O_3-$YFe_2O_{4-x'''}$-$YFeO_3$	$-\frac{39375}{T} + 20.43 \pm 0.04$	(7)
F $Fe_{1-y''}O$-YFe_2O_4-$YFeO_3$	$-\frac{45325}{T} + 25.64 \pm 0.05$	(8)
G $Fe_{1-y'''}O$-Fe_3O_4-$YFeO_3$	$-\frac{33245}{T} + 18.45 \pm 0.04$	(9)
H Fe_3O_4-$YFeO_3$-$Y_3Fe_5O_{12}$	$-\frac{26365}{T} + 17.13 \pm 0.06$	(10)

It is noted that regions C and D have the same oxygen activity because they are both bounded by the same Fe-$Fe_{1-y}O$ 2-phase region on the Fe-O leg of the Gibbs triangle and the amount of the third compound $YFeO_3$ or YFe_2O_{4-x}, respectively, is not changed during oxidation or reduction.

It may be seen from Fig. 4 that the two lines C and A branch at points a and b, respectively, where neighbouring 3-phase regions approach the same

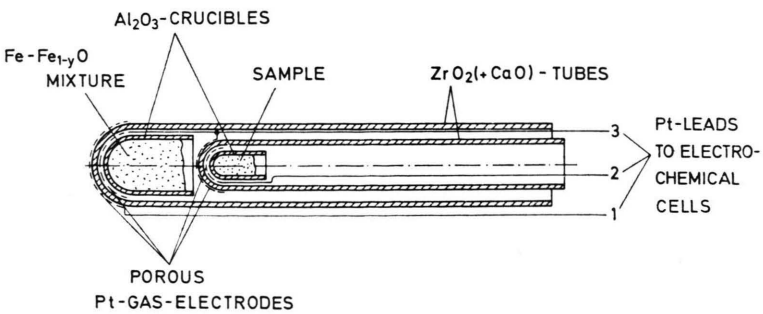

Fig. 3. Experimental arrangement of the galvanic cell with an auxiliary $Fe + Fe_{1-y}O$ electrode.

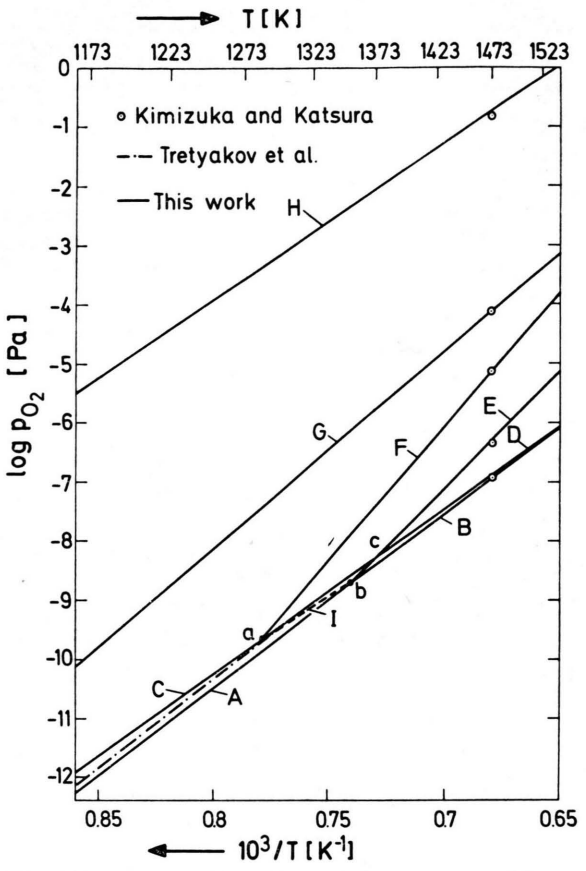

Fig. 4. Temperature dependence of the oxygen equilibrium pressures of the various 3-phase regions in the Y—Fe—O system. The capital numbers are explained in Table 1. The broken line I is estimated for the 3-phase region Fe—$YFeO_3$—YFe_2O_{4-x}'.

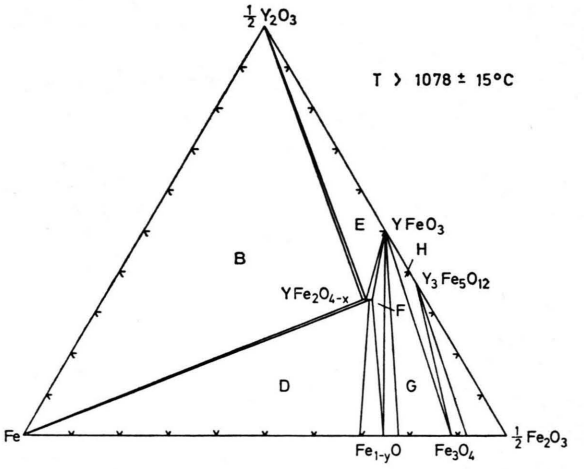

Fig. 5. Equilibrium phase diagram of the partial system Fe—Fe_2O_3—Y_2O_3 at temperatures above 1078 °C.

oxygen equilibrium pressures. Under the conditions indicated by *a* ((1010 ± 9) °C, $\log p_{O_2}$[Pa] = −9.68 ± 0.05) the four solid phases Fe, $Fe_{1-y}O$, YFe_2O_{4-x} and $YFeO_3$ can be in equilibrium simultaneously. Likewise, at point *b* ((1078 ± 15) °C, $\log p_{O_2}$[Pa] = −8.71 ± 0.05) Fe, Y_2O_3, YFe_2O_{4-x} and $YFeO_3$ can co-exist simultaneously in equilibrium in the solid state. According to the phase rule, the system at those points has no degree of freedom anymore. Points *a* and b are therefore invariant points of the system.

Figure 5 shows the phase diagram of the system Fe-Fe_2O_3-Y_2O_3 obtained at temperatures above (1078 ± 15) °C. Y_2O_3 is in equilibrium with YFe_2O_{4-x} in this temperature region as indicated by the 2-phase region connecting these compositions. The phase diagram is in accordance with the results obtained by Kimizuka and Katsura [6] at 1200 °C.

Below (1078 ± 15) °C Y_2O_3 and YFe_2O_{4-x} are no longer in equilibrium and $YFeO_3$ and Fe may co-exist instead. The phase diagram as shown in Fig. 6 is observed. It is valid for the temperature range from (1010 ± 9) °C to (1078 ± 15) °C.

Below (1010 ± 9) °C the 2-phase regions connecting YFe_2O_{4-x} with Fe, $YFeO_3$ and $Fe_{1-y}O$ will disappear. The oxygen equilibrium pressures of all 3-phase regions D, F, and I around YFe_2O_{4-x} become equal. YFe_2O_{4-x} cannot exist anymore as a stable phase at temperatures below (1010 ± 9) °C. It decomposes into Fe, $Fe_{1-y}O$ and $YFeO_3$. The

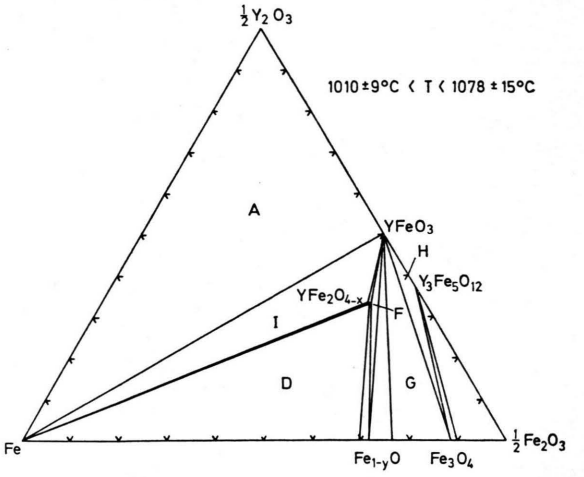

Fig. 6. Equilibrium phase diagram of the partial system Fe—Fe_2O_3—Y_2O_3 in the temperature range from 1010 to 1078 °C.

phase diagram transforms into the one shown in Figure 7.

At point *c* ((1098 ± 13) °C, $\log p_{O_2}$[Pa] = −8.29 ± 0.04) two lines intersect which represent the oxygen partial pressure of two 3-phase regions without common boundaries in the phase diagram. This has no implications on the phase diagram.

3.2. Thermodynamic Calculations

The reactions

$$1/2\ Y_2O_3 + Fe + 3/4\ O_2 = YFeO_3 \qquad (11)$$

and

$$3\ YFeO_3 + 2/3\ Fe_3O_4 + 1/6\ O_2 = Y_3Fe_5O_{12} \qquad (12)$$

have been studied in our previous paper [8] and the corresponding Gibbs (free) energies of reactions have been determined to be

$$\Delta G^0_{(11)} = (-421.3 + 0.1184 \times T \pm 0.7)\ \text{kJ/mol} \quad (1173 \leqq T[\text{K}] \leqq 1523) \qquad (13)$$

and

$$\Delta G^0_{(12)} = (-84.1 + 0.0387 \times T \pm 0.2)\ \text{kJ/mol} \quad (1173 \leqq T[\text{K}] \leqq 1523). \qquad (14)$$

In order to calculate the standard Gibbs energies of formation of yttrium iron perovskite, ΔG_f^0 ($YFeO_3$), and yttrium iron garnet, ΔG_f^0 ($Y_3Fe_5O_{12}$), the thermodynamic properties of Y_2O_3 and Fe_3O_4 have to be known. The data for magnetite are well established [12] whereas discrepancies exist in the case of yttria. In contrast to thermodynamic tables [12], Y_2O_3 exists only in the C-type rare-earth sesquioxide modification [13] in the relevant temperature range. We have selected from Gmelin's Handbook [14]:

$$\Delta H^0_{f,\,298.15}(Y_2O_3) = -1905.6\ \text{kJ/mol},$$
$$S^0_{298.15}(Y_2O_3) = 99.12\ \text{J/mol} \cdot \text{K},$$
$$c_p{}^0(Y_2O_3) = (11.78 + 14.64 \times 10^{-3} \times T - 17.45 \times 10^5 \times T^{-2})\ \text{J/mol} \cdot \text{K} \quad (298 \leqq T[\text{K}] \leqq 1615).$$

With the help of these data the standard Gibbs energies of formation can be expressed by the following equations which are linear within the experimental error:

$$\Delta G_f{}^0(YFeO_3) = (-1366.0 + 0.2525 \times T \pm 0.7)\ \text{kJ/mol} \quad (1173 \leqq T[\text{K}] \leqq 1523), \qquad (15)$$

$$\Delta G_f{}^0(Y_3Fe_5O_{12}) = (-4912.2 + 0.9990 \times T \pm 2.3)\ \text{kJ/mol} \quad (1173 \leqq T[\text{K}] \leqq 1523). \qquad (16)$$

The indicated errors include both the standard deviations of the cell voltage and the inaccuracy of the temperature measurement. Errors due to data taken from the literature are not considered. The same holds for all other results presented in this paper.

From the temperature dependence, the standard enthalpies of formation, $\Delta H_f{}^0$, and standard entropies of formation, $\Delta S_f{}^0$, are obtained to be

$$\Delta H_f{}^0(YFeO_3) = (-1366.0 \pm 0.7)\ \text{kJ/mol} \quad (1173 \leqq T[\text{K}] \leqq 1523), \qquad (15a)$$

$$\Delta S_f{}^0(YFeO_3) = (-252.5 \pm 4.0)\ \text{J/mol} \cdot \text{K} \quad (1173 \leqq T[\text{K}] \leqq 1523), \qquad (15b)$$

$$\Delta H_f{}^0(Y_3Fe_5O_{12}) = (-4912.2 \pm 2.3)\ \text{kJ/mol} \quad (1173 \leqq T[\text{K}] \leqq 1523), \qquad (16a)$$

$$\Delta S_f{}^0(Y_3Fe_5O_{12}) = (-999.0 \pm 13.05)\ \text{J/mol} \cdot \text{K} \quad (1173 \leqq T[\text{K}] \leqq 1523). \qquad (16b)$$

Making use of these results and the present experimental data we are able to determine also the Gibbs energy of formation of the compound YFe_2O_4.

According to Eqs. (2) and (3) the cell voltage of the 3-phase region $YFeO_3$-$Fe_{1-y}O$-YFe_2O_4 (F)

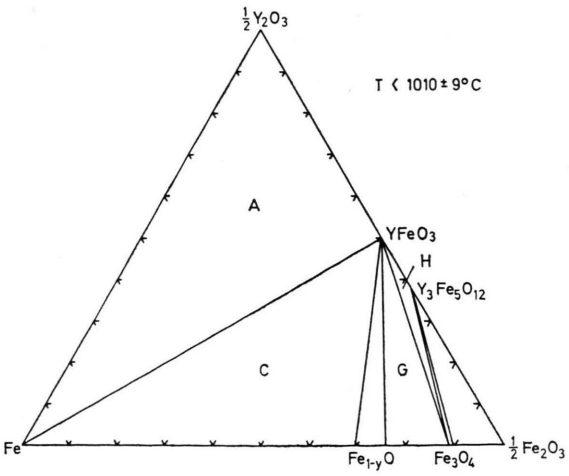

Fig. 7. Equilibrium phase diagram of the partial system $Fe-Fe_2O_3-Y_2O_3$ at temperatures below 1010 °C.

with reference to a pure oxygen electrode of atmospheric pressure is given by

$$E = -\frac{1}{2F\,y''}\left[(1-y'')\,\Delta G_f^0(\mathrm{YFeO_3}) + \Delta G_f^0(\mathrm{Fe_{1-y''}O}) - (1-y'')\,\Delta G_f^0(\mathrm{YFe_2O_4})\right]. \quad (17)$$

This equation takes into account the fact that YFe_2O_4 has practically ideal stoichiometric composition ($x=0$) if it is in equilibrium with $YFeO_3$ and $Fe_{1-y''}O$ [6]. Also, the solubility of $YFeO_3$ and YFe_2O_{4-x} may be assumed to be negligibly small in wuestite [6]. The same holds for the solubility of $Fe_{1-y}O$ and YFe_2O_{4-x} in the stoichiometric perovskite $YFeO_3$.

Solving Eq. (17) for the Gibbs energy of formation of YFe_2O_4 and substituting the cell voltage E by the oxygen equilibrium pressure of the 3-phase region F according to Eqs. (1) and (2), yields

$$\Delta G_f^0(\mathrm{YFe_2O_4}) = -\frac{RT}{2(1-y'')}\ln p_{O_2}(F) + \Delta G_f^0(\mathrm{YFeO_3}) - \frac{1}{(1-y'')}\Delta G_f^0(\mathrm{Fe_{1-y''}O}). \quad (18)$$

$\Delta G_f^0(Fe_{1-y''}O)$ may be determined by integration of the cell voltage (with reference to a pure oxygen electrode of atmospheric pressure) as a function of the oxygen content along the tie line (co-ordinate z) connecting the Fe corner of the Gibbs triangle and the composition $Fe_{1-y''}O$ [11]

$$\Delta G_f^0(\mathrm{Fe_{1-y''}O}) = -2(1-y'')\,F\int_0^{1/(1-y'')} E(z)\,\mathrm{d}z = \frac{(1-y'')\,RT}{2}\int_0^{1/(1-y'')} \ln p_{O_2}(z)\,\mathrm{d}z. \quad (19)$$

The cell voltage or equilibrium oxygen partial pressure of the 2-phase mixture of Fe and $Fe_{1-y'}O$ can be taken from the literature [15—22]. Data taken from Refs. [17, 18, 21, 22] are in very good agreement with the results obtained in our study for the regions C and D in which the third compound does not influence the voltage since its solubility is negligibly small and its amount is not changed during the process of variation of the oxygen concentration. Therefore, we have employed Eq. (6) for the integration along the 2-phase region Fe-$Fe_{1-y'}O$. With regard to the single phase region $Fe_{1-y}O$ it is known that its stoichiometric deviation varies nearly linearly with the cell voltage E or the logarithm of the equilibrium oxygen pressure [21, 23]. The integration was carried out according to this stoichiometric dependence up to the oxygen partial pressure of the region F as expressed by Equation (8). The result of this calculation is

$$\Delta G_f^0(\mathrm{YFe_2O_4}) = (-1615.9 + 0.3068\times T \pm 2.5)\ \mathrm{kJ/mol} \quad (1283 \leqq T[\mathrm{K}] \leqq 1523). \quad (20)$$

From this expression, the standard enthalpy of formation, ΔH_f^0, and the standard entropy of formation, ΔS_f^0, are obtained to be

$$\Delta H_f^0(\mathrm{YFe_2O_4}) = (-1615.9 \pm 2.5)\ \mathrm{kJ/mol} \quad (1283 \leqq T[\mathrm{K}] \leqq 1523), \quad (21)$$

and

$$\Delta S_f^0(\mathrm{YFe_2O_4}) = (-306.8 \pm 20.8)\ \mathrm{J/mol\cdot K} \quad (1283 \leqq T[\mathrm{K}] \leqq 1523), \quad (22)$$

respectively. Further thermodynamic data may be derived from these results by employing known thermodynamic relationships.

4. Discussion

The applied electrochemical technique has been proved to be a powerful, highly precise and elegant tool for the determination of the phase diagram and the thermodynamics of the ternary system Y-Fe-O.

The results obtained in this work confirm the measurements of Kimizuka and Katsura [6] performed at 1200 °C. The differences in the logarithms of the oxygen equilibrium pressures of all 3-solid-phase regions at this temperature are very small and fall within the limit of the experimental error.

Moreover, the oxygen equilibrium pressures of the regions Fe-$Fe_{1-y}O$-$YFeO_3$ (C) and Fe-$Fe_{1-y}O$-YFe_2O_{4-x} (D) agree well with the data reported for the Fe-$Fe_{1-y}O$ system. In contrast, the oxygen equilibrium pressures of the Y_2O_3-Fe-$YFeO_3$ region (A) are lower than those obtained by Tretyakov et al. [7]. The oxygen equilibrium pressures of the $Fe_{1-y}O$-Fe_3O_4-$YFeO_3$ region (G) are consistent with the data given in [19] for the $Fe_{1-y}O$-Fe_3O_4 system. However, the agreement with other published data is poor and it should be emphasized that the differences are greater than our experimental error.

[1] J. W. Nielsen and E. F. Dearborn, Phys. Chem. Solids **5**, 202 (1958).
[2] H. J. Van Hook, J. Amer. Ceram. Soc. **44**, 208 (1961).
[3] J. Cassedane, C. R. Acad. Sci. Paris **252**, 3261 (1961).
[4] H. J. Van Hook, J. Amer. Ceram. Soc. **45**, 162 (1962).
[5] H. J. Van Hook, J. Amer. Ceram. Soc. **46**, 248 (1963).
[6] N. Kimizuka and T. Katsura, J. Solid State Chem. **13**, 176 (1975).
[7] Yu. D. Tretyakov, A. R. Kaul, and V. K. Portnoy, High Temp. Sci. **9**, 61 (1977).
[8] W. Piekarczyk, W. Weppner, and A. Rabenau, Mat. Res. Bull. **13**, 1077 (1978).
[9] Chen Li-chuan and W. Weppner, Naturwiss. **65**, 595 (1978).
[10] W. Weppner, Chen Li-chuan, and A. Rabenau, submitted to J. Solid State Chem.
[11] W. Weppner, Chen Li-chuan, and W. Piekarczyk, submitted to J. Amer. Ceram. Soc.
[12] I. Barin and O. Knacke, Thermochemical Properties of Inorganic Substances, Springer, Berlin 1973; I. Barin, O. Knacke, and O. Kubaschewski, Thermochemical Properties of Inorganic Substances, Supplement, Springer, Berlin 1977.
[13] R. P. Elliot, Constitution of Binary Alloys, First Supplement, McGraw-Hill, New York 1965.
[14] Gmelins Handbuch der anorganischen Chemie, Syst.-No. 39, Part C 1, Springer, Berlin 1974.
[15] L. S. Darken and R. W. Gurry, J. Amer. Chem. Soc. **67**, 1398 (1945).
[16] L. S. Darken and R. W. Gurry, J. Amer. Chem. Soc. **68**, 798 (1946).
[17] G. G. Charette and S. N. Flengas, J. Electrochem. Soc. **115**, 796 (1968).
[18] J. Moriyama, N. Sato, H. Asao, and Z. Kozuka, Mem. Fac. Eng., Kyoto Univ. **31**, 253 (1969).
[19] H. F. Rizzo, R. S. Gordon, and I. B. Cutler, J. Electrochem. Soc. **116**, 266 (1969).
[20] Y. Saito, K. Nishimura, J. Sakamoto, T. Yamamura, and Y. Iwano, J. Japan Soc. Powder Metal. **18**, 229 (1972).
[21] H. Rickert and W. Weppner, Z. Naturforsch. **29a**, 1849 (1974).
[22] Su-Il Pyun and F. Müller, High Temp. High Press. **9**, 111 (1977).
[23] I. Bransky and A. Z. Hed, J. Amer. Ceram. Soc. **51**, 231 (1968).